

Universality of the SIS prevalence in networks

P. Van Mieghem*

5 December 2016: for Nathan's birthday

Abstract

Epidemic models are increasingly used in real-world networks to understand diffusion phenomena (such as the spread of diseases, emotions, innovations, failures) or the transport of information (such as news, memes in social on-line networks). A new analysis of the prevalence, the expected number of infected nodes in a network, is presented and physically interpreted. The analysis method is based on spectral decomposition and leads to a universal, analytic curve, that can bound the time-varying prevalence in any finite time interval. Moreover, that universal curve also applies to various types of Susceptible-Infected-Susceptible (SIS) (and Susceptible-Infected-Removed (SIR)) infection processes, with both homogenous and heterogeneous infection characteristics (curing and infection rates), in temporal and even disconnected graphs and in SIS processes with and without self-infections. The accuracy of the universal curve is comparable to that of well-established mean-field approximations.

1 Introduction to SIS epidemics on networks

Epidemic processes on a network can approximately describe an amazingly large variety of real-world processes [1], such as the spread of a disease, a digital virus, a message in an on-line social network, an emotion, the propagation of a failure or an innovation and other diffusion phenomena on networks (competing opinions, social contagion [2]). While the study of epidemics dates back to the great Bernoulli's, the investigation of the role of the underlying graph on the dynamics of the susceptible-infected-susceptible (SIS) process was only initiated 15 years ago with the seminal paper of Pastor-Satorras and Vespignani [3]. The relatively new field of network science [4, 5, 6, 7, 8, 9] aims to study the interplay between dynamic processes on a graph and the characteristics of that underlying graph. In [10], we discussed the “Local rule-Global emergent properties” (LrGep) class, where the collective action of the local rules executed at each node in the network gives rise to a complex, emergent global network behavior. Prominent examples of the LrGep-class are epidemic models and more general reaction-diffusion processes [1], the Ising spin model [11], the Kuramoto coupled-oscillator model [12], cellular automata [13], sandpiles as models for self-organized criticality [14, 15, 16] and opinion models [17, 18]. The fascinating binding of these LrGep class members is that many LrGep models feature a phase transition [19], they all depend heavily on the underlying topology and many processes in nature seem well described by LrGep models. The simplicity of the local rules disguises the overwhelming

*Delft University of Technology, Faculty of EECS, P.O Box 5031, 2600 GA Delft, The Netherlands; *email*: P.F.A.VanMieghem@tudelft.nl

complexity of the global emergent network behavior that these local rules create. Even one of the simplest members of the LrGep class, the SIS process, is intricate and not sufficiently understood. However, the Markovian SIS process on networks allows for the highest degree of analytic treatment, which is a major motivation for the continued effort towards its satisfactory understanding. Here, we report on a universal property of the SIS prevalence and we propose a new analytic approximation with an accuracy comparable to the well-established mean-field models [1].

We consider an unweighted, undirected graph G containing a set \mathcal{N} of N nodes and a set \mathcal{L} of L links. The topology of the graph G is represented by a symmetric $N \times N$ adjacency matrix A . In an SIS epidemic process [20, 21, 22, 23, 1, 24], the viral state of a node i at time t is specified by a Bernoulli random variable $X_i(t) \in \{0, 1\}$: $X_i(t) = 0$, when node i is healthy, but susceptible and $X_i(t) = 1$, when node i is infected. A node i can only be in one of these two states: *infected*, with probability $\Pr[X_i(t) = 1]$ or *healthy*, with probability $\Pr[X_i(t) = 0]$, but susceptible to the infection. We assume that the curing process for node i is a Poisson process with rate δ_i and that the infection rate over the link (i, j) is a Poisson process with rate β_{ij} . Only when node i is infected, it can infect each node k of its healthy direct neighbors with rate β_{ik} . All Poisson curing and infection processes are independent. This description defines the continuous-time, Markovian *heterogeneous* SIS epidemic process on a graph G . We do not consider non-Markovian epidemics [25, 26] and assume that the infection characteristics in the graph, i.e. all curing and infection rates, are independent of time. The fraction of infected nodes is defined as

$$S(t) = \frac{1}{N} \sum_{i=1}^N X_i(t) \quad (1)$$

and its expectation, called the *prevalence* or the order parameter, equals

$$y(t) = E[S(t)] = \frac{1}{N} \sum_{i=1}^N \Pr[X_i(t) = 1] \quad (2)$$

exploiting the property $E[X_i] = \Pr[X_i = 1]$ of a Bernoulli distribution, which enables to avoid computations with the probability operator in favor of the easier, linear expectation operator. In that setting, the exact Markovian *heterogeneous* SIS governing equation [27, 8] for the infection probability of node i is

$$\frac{dE[X_i(t)]}{dt} = E \left[-\delta_i X_i(t) + (1 - X_i(t)) \sum_{k=1}^N \beta_{ki} a_{ki} X_k(t) \right] \quad (3)$$

When node i is infected at time t and $X_i(t) = 1$, only the first term on the right-hand side between the brackets $[\cdot]$ affects and decreases with rate $-\delta_i$ the change in infection probability with time $\frac{d\Pr[X_i(t)=1]}{dt}$ (left-hand side in (3)). When node i is healthy, $X_i(t) = 0$ and $(1 - X_i(t)) = 1$, only the second term between the brackets $[\cdot]$ increases $\frac{d\Pr[X_i(t)=1]}{dt}$ by a rate $\sum_{k=1}^N \beta_{ki} a_{ki} X_k(t)$ due to all its infected, direct neighbors. We define the Bernoulli random vector $w(t) = (X_1(t), X_2(t), \dots, X_N(t))$ at time t , the nodal curing vector $\tilde{\delta} = (\delta_1, \delta_2, \dots, \delta_N)$ and the weighted adjacency matrix \tilde{A} with element $\tilde{a}_{ij} = \beta_{ij} a_{ij}$, that can change with time t as in temporal networks [28]. If $\beta_{ki} = \beta_{ik}$, the corresponding *heterogeneous* SIS prevalence differential equation is (see Theorem 1 in Appendix A)

$$N \frac{dy(t)}{dt} = -E \left[\tilde{\delta}^T w(t) \right] + E \left[(w(t))^T \tilde{Q}(t) w(t) \right] \quad (4)$$

where the time-dependent, weighted Laplacian $\tilde{Q}(t) = \tilde{\Delta}(t) - \tilde{A}(t)$ is an $N \times N$ positive semi-definite symmetric matrix, with the diagonal matrix $\tilde{\Delta}(t) = \text{diag}(\tilde{d}_1, \tilde{d}_2, \dots, \tilde{d}_N)$ and the infection strength of node k is $\tilde{d}_k = \sum_{i=1}^N \beta_{ki} a_{ki}$. In a *homogeneous* SIS process, where all $\beta_{ij} = \beta$ and $\delta_j = \delta$, (4) simplifies [29] to,

$$\frac{dy(t^*; \tau)}{dt^*} = -y(t^*; \tau) + \frac{\tau}{N} E \left[w(t^*; \tau)^T Q w(t^*; \tau) \right] \quad (5)$$

where $\tau = \frac{\beta}{\delta}$ is the effective infection rate, $t^* = t\delta$ is the normalized time, $Q = \Delta - A$ is the Laplacian of the graph G with $\Delta = \text{diag}(d_1, d_2, \dots, d_N)$ and d_i is the degree of node i . The corresponding governing equation for the prevalence of the SIR process is deduced in [30]. Assume in a temporal network that the infection characteristics do not change, but only links in the graph change at time t : $A(t - \varepsilon) = A_1$ and $A(t + \varepsilon) = A_2$ for any arbitrarily small real $\varepsilon > 0$. Since the number N of nodes does not change, the number of infected nodes is continuous at time t . Thus, the Bernoulli vector $w(t) = \lim_{\varepsilon \rightarrow 0} w(t - \varepsilon) = \lim_{\varepsilon \rightarrow 0} w(t + \varepsilon)$ is continuous at time t and the prevalence differential equation (4) shows that

$$\left. \frac{dy(t)}{dt} \right|_{t+\varepsilon} - \left. \frac{dy(t)}{dt} \right|_{t-\varepsilon} = \frac{1}{N} E \left[(w(t))^T (\tilde{Q}_2 - \tilde{Q}_1) w(t) \right] \quad (6)$$

implying that the derivative of the prevalence is likely not continuous at the time when the topology changes. On the other hand, the derivative $\frac{dy(t)}{dt}$ is continuous when the topology does not change (nor the infection characteristics). Thus, the SIS prevalence on temporal networks may show a discontinuous slope at time t , from which a topology change at that time t may be inferred.

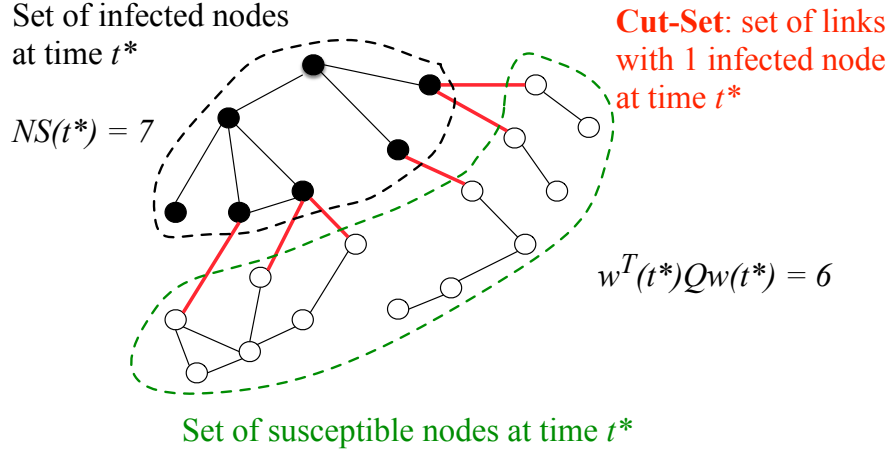


Figure 1: A sketch of an epidemic state in a graph at time t^* , described by (5), illustrates the three sets: (a) the set of infected nodes containing $NS(t^*) = 7$ nodes (in black), (b) the set of susceptible nodes (in green) and (c) the cut-set (in red): the number of links with one infected node and here equal to $w^T(t^*)Qw(t) = 6$ links.

2 The cut-set

The evolution of the nodal infection, described by (3), reflects the “local rule” of the SIS process, whereas the SIS prevalence differential equation (4) describes the “global emergent properties”. In (3), (4) and (5), the second, non-linear term quantifies the coupling between process and underlying topology. Fig. 1 illustrates that this physical interaction is embedded in the cut-set $(w(t))^T Qw(t)$, which equals the number of links with one end node infected at time t . Given that one node is infected initially and that the effective infection rate τ is well above the epidemic threshold τ_c , the early infection spreads as the ripples in a pool caused by throwing a stone in the water. First the direct neighbors become infected, then the neighbors of those neighbors and so on. This early spread can be specified by the *expansion* of the graph [8, p. 371], a graph metric which determines the number of nodes at k hops from the initial node. In this early phase, the epidemic grows exponentially with time and the cut-set boundary is analogous to “concentric circles in a pool” around the initially infected node [31]. After some time, infected nodes cure and move in Fig. 1 to the set of susceptible nodes. When the number of successive shells around the initial node exceeds the average hopcount [8, p. 360 & Chapter 16], i.e. number of links of the shortest path between two arbitrary nodes, the finite size of the graph prevents exponential increase in the number of nodes reached from an initial node. Hence, two effects, curing and finite graph structure, limit the growth of an epidemic. After the early phase, the cut-set as well as its border line between infected and healthy nodes cease to resemble simple geometric concentric circles and start exhibiting a complicated shape. Determining the largest cut-set, which corresponds to the fastest possible viral increase (see (4)) in the network, is NP-hard, as well as finding the smallest cut-size that is related [32, p. 95] to the isoperimetric constant η , which upper bounds the epidemic threshold $\tau_c \leq \frac{1}{\eta}$, as shown by Ganesh *et al.* [33]. In spite of its computational difficulty, the key to understanding an infectious spread lies in the cut-set, which is the place to prevent epidemic spread. The latest dynamic control strategies [34] target the reduction of the cut-set $(w(t))^T Qw(t)$ at each time t .

3 Universality of the tanh-formula

Our major new result concerns “universality”: the time-varying prevalence $y(t)$ of any Markovian SIS process, be it homogeneous or heterogeneous in its infection or/and curing rates, in temporal or even disconnected graphs, with or without self-infections, can be upper and lower bounded by a single, universal curve. To simplify the explanation, we concentrate on a homogeneous SIS process and refer to Appendices E and F for the other cases.

Our method, which is *entirely different from the mean-field concept*, is based on the spectral decomposition of the cut-set $(w(t))^T Qw(t)$ and of the Bernoulli state vector w , whose components $w_j = X_j$ are only zero or one. Physically, the dynamics (5) of the SIS epidemics, characterized by the Bernoulli vector w and the Laplacian matrix Q , is mapped onto the Laplacian eigenspace, determined by the underlying graph G . As shown in Appendix C, the Bernoulli vector w is projected onto the N orthogonal axes formed by the real, normalized Laplacian eigenvectors x_1, x_2, \dots, x_N belonging to the eigenvalues $\mu_1 \geq \mu_2 \geq \dots \geq \mu_N = 0$, respectively, and obeying the orthogonality condition $x_k^T x_m = 1$ if $k = m$, otherwise $x_k^T x_m = 0$. The coordinates in the Laplacian eigenvector basis, $\zeta_j = w^T x_j$ for

$1 \leq j \leq N$, completely specify the Bernoulli vector w . The relative success of the method is, in contrast to the adjacency matrix, due to the knowledge of one eigenvector $x_N = \frac{1}{\sqrt{N}}u$ belonging to the eigenvalue $\mu_N = 0$ and where $u = (1, 1, \dots, 1)$ is the all-one vector. The corresponding coordinate is $\zeta_N = \frac{1}{\sqrt{N}}u^T w = \sqrt{N}S$, by the definition (2) written in vector form as $S = \frac{u^T w}{N}$. Since w is a zero-one vector, the largest scalar product $\zeta_j = w^T x_j$ is ζ_N , which means that the Bernoulli vector w is most close to the eigenvector x_N . In addition, the norm of the Bernoulli vector equals the sum of its components, $w^T w = u^T w = NS$, which allows to specify the second most influential coordinate ζ_{N-1} .

We consider a graph G consisting of k connected components, where the k smallest Laplacian eigenvalues are zero, but $\mu_{N-k} > 0$ (see Appendix B). For a connected graph ($k = 1$), the second smallest eigenvalue $\mu_{N-1} > 0$ of the Laplacian Q , coined by Fiedler [35] the algebraic connectivity, is studied over the last decades [32]. After spectral decomposition, the differential equation (5) becomes

$$\frac{dy(t^*; \tau)}{dt^*} = (\tau\mu_{N-k} - 1)y(t^*; \tau) - \tau\mu_{N-k}y^2(t^*; \tau) - \Psi_k(t^*; \tau) \quad (7)$$

where the remainder $\Psi_k(t^*; \tau)$ is explicitly given in (21). If $\Psi_k(t^*; \tau)$ equals a constant c , then (7) reduces to a Riccati differential equation, which can be solved exactly. Assuming that we can bound $\Psi_k(t^*; \tau)$ in a normalized time interval $[t_1^*, t_2^*]$ by two constants, $c_L(k) \leq \Psi_k(t^*; \tau) \leq c_U(k)$, then the prevalence $y(t^*)$ can be bounded in $[t_1^*, t_2^*]$, for the same initial condition y_0 , by

$$T(t^* | y_0, \tau\mu_{N-k}, c_U(k)) \leq y(t^*) \leq T(t^* | y_0, \tau\mu_{N-k}, c_L(k))$$

where our ‘‘tanh-formula’’ is

$$T(t | y_0, s, c) = \frac{1}{2} \left(1 - \frac{1}{s} \right) + \frac{\Xi}{2} \tanh \left(\frac{s\Xi}{2} t + \Omega_0 \right) \quad (8)$$

with the Laplacian normalized effective infection rate $s = \tau\mu_{N-k}$ and

$$\Omega_0 = \operatorname{arctanh} \left(\frac{2y_0 - (1 - \frac{1}{s})}{\Xi} \right) \quad (9)$$

and

$$\Xi = \sqrt{\left(1 - \frac{1}{s} \right)^2 - \frac{4c}{s}} \quad (10)$$

Fig. 2 draws the tanh-formula (8) as a function of normalized time t^* for various $c \in [-1, 0]$, in two characteristic regimes above ($\tau\mu_{N-k}$ high) and below ($\tau\mu_{N-k}$ small) the epidemic threshold.

We argue in Appendix D that, for $k = 1$, a rough estimate for $c \approx -y_0$. Our tanh-formula (8) approximates the total contribution $\Psi_k(t^*; \tau)$, containing the less influential Bernoulli vector coordinates in the Laplacian eigenspace, by a constant c . Extensive simulations [36] on various graph types and infection characteristics, compared with the N -Intertwined Mean-Field Approximation (NIMFA, [37]), demonstrate that the tanh-formula (8) has an overall performance comparable to mean-field approximations.

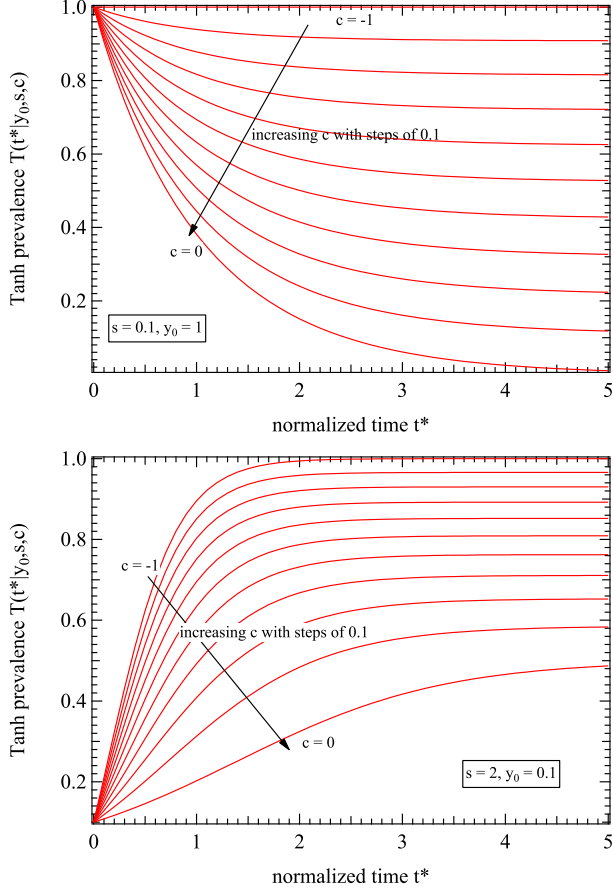


Figure 2: The tanh-formula (8) as a function of normalized time t^* for various values of $c = \{-1, -0.9, -0.8, \dots, 0\}$. Two characteristic regimes are shown: (above) $s = \tau\mu_{N-k}$ below the epidemic threshold and initial condition $y_0 = 1$, where all are nodes infected, and (below) $s = \tau\mu_{N-k}$ above the epidemic threshold and initial condition $y_0 = 0.1$.

4 Potential of the tanh-formula (8)

We discuss the tanh-formula (8) further. First, (8) contains three parameters: the initial condition y_0 , $s = \tau\mu_{N-k}$ and c that all depend upon the underlying graph. Remarkably, the expectation of a complicated dynamic process – the prevalence is an expectation – is approximately characterized by only three parameters. Second, the tanh-formula (8) generalizes the classical Kermack and McKendrick expression of 1927 by incorporating the graph. Assuming “homogeneous mixing”, equivalent to regarding the underlying network as a complete graph K_N , Kermack and McKendrick [38] demonstrated that the SIR prevalence is described by the time-derivative of a simplified variant of our tanh-formula (8). The correspondence with our tanh-formula (8) is not so surprising: in the complete graph K_N with algebraic connectivity $\mu_{N-1} = N$, the complicated remainder reduces to its simplest possible form: $\Psi_1(t^*; \tau) = \tau N \text{Var}[S(t^*; \tau)]$. In K_N , the fraction of infected nodes $S(t^*; \tau)$ is close to a Gaussian random variable [39] above the epidemic threshold τ_c and the variance $\text{Var}[S(t^*; \tau)] \approx \frac{1}{N}$ is almost constant in the metastable regime. Generally, in sufficiently large networks and above the epidemic

threshold, the average total infection “force” is balanced in equilibrium by the average total healing “force” and the individual infection state X_j of node j is only weakly dependent on X_k of node k . Under these conditions of weakly dependence, the Central Limit Theorem [8] states that the fraction S of infected nodes tends to a Gaussian with mean $y = E[S]$ and standard deviation $\sigma = \sqrt{\text{Var}[S]}$. The tanh-formula (8) does not include the eventual die-out of the SIS epidemic in any finite network. Once the epidemic has reached the metastable state in which the two above mentioned forces balance each other on average, small process fluctuations of a couple of standard deviations σ around the mean y continuously occur, but large fluctuations are rare. In the metastable, a die-out of the SIS process can only be caused by a cascade of mainly curing events in succession, which is a very rare event. Consequently, once the process has reached the metastable state, the epidemic remains in the network for a very long time [40, 41, 42], which practically means for large real-world networks that the SIS epidemics remains in the metastable state. Hence, for large N and for effective infection rates $\tau > \tau_c$, the tanh-formula (8) models the “real” SIS epidemic very well, although it ignores absorption. Third, the parameter c approximates the complicated remainder $\Psi_k(t^*; \tau)$. The important bounding

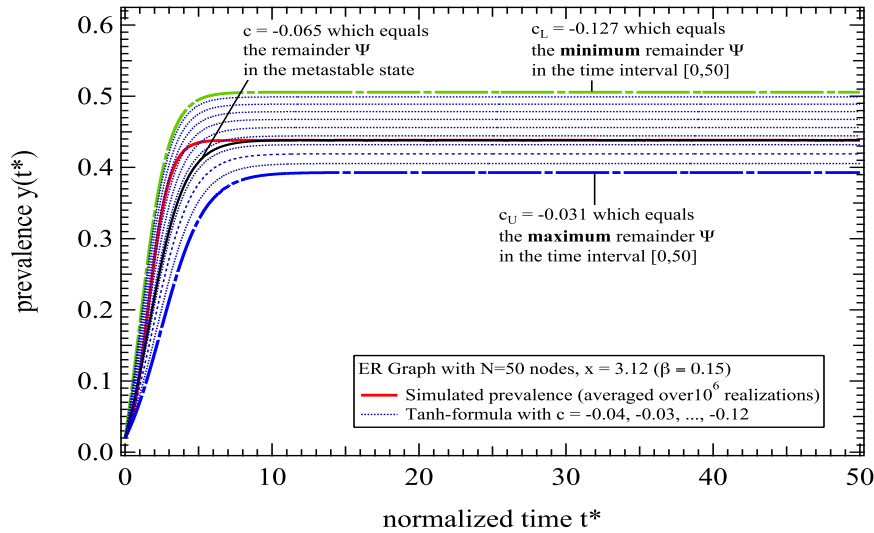


Figure 3: The prevalence envelope in a normalized time interval $[0, 50]$ for an instance of an Erdős-Rényi random graph $G_p(N)$ with $N = 50$ nodes, link density $p = 0.4$ and spectral radius $\lambda_1 = 20.8$. Initially, one random node was infected. The infection rate $\beta = 0.15$ and the curing rate $\delta = 1$, leading to a normalized effective infection rate $x = \frac{\tau}{\tau_c^{(1)}} = \lambda_1 \tau = 3.12$.

assumption $c_L(k) \leq \Psi_k(t^*; \tau) \leq c_U(k)$ leads to the prevalence envelope, illustrated in Fig. 3 and akin to [43], which encloses (see also Fig. 4) roughly 68% of all realizations (i.e. all possible real-world measurements of an SIS epidemic) assuming Gaussian fluctuations around the prevalence – which is, as mentioned above, a good approximation for dense graphs as K_N sufficiently above the epidemic threshold. In absence of sufficiently clean data of a real-world SIS prevalence, Fig. 4 plots 50 random realizations of $S(t^*)$ out of 10^6 with the same infection characteristics and on the same graph as in Fig. 3. Since only the realizations that have reached the metastable state after a start with one initially infected, randomly chosen node, are observable, the prevalence is rescaled to $y = \frac{N_m y_m + N_d y_d}{N} = \frac{N_m}{N} y_m$,

where the index m refers to those realizations that reach the metastable state, and d those that die out fast [44] and never reach the metastable state. Usually, the die-out probability, given an initial number of infected nodes, is unknown, which complicates, as demonstrated in Fig. 4 the proper normalization in reality, where often only one realization of a spreading process (e.g. of a disease) is measured over time. Fortunately, NIMFA [29] upper bounds the prevalence, ignoring that realizations die out, while the tanh-formula (8) can fit, upper or lower bound data to infer from the parameters $(y_0, \tau\mu_{N-k}, c)$ insights in the epidemic.

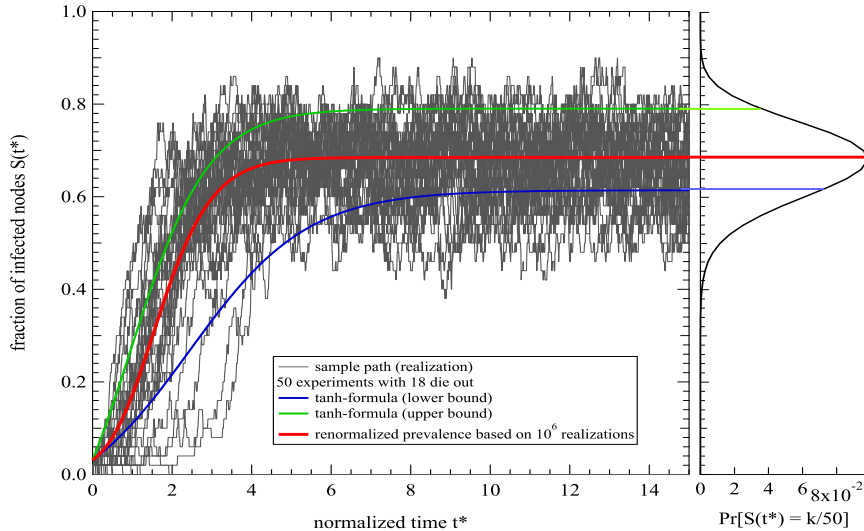


Figure 4: A random selection of 50 realizations out 10^6 realizations, shown in Fig. 3. Conditioned on 28 realization that did not die out, the prevalence (red) has been renormalized as well as the tanh-formula (8) upper (green) and lower bound (blue) in Fig. 3

Fourth, the tanh-formula (8) can be used in temporal networks by gluing the different time-regimes in which the network is unaltered: at time t , where the topology changes, we impose continuity in the prevalence, $y(t-\varepsilon) = y(t+\varepsilon)$ for $\varepsilon \rightarrow 0$, but allow discontinuity in the derivatives as in (6). The tanh-formula (8) is the more accurate, the better $\Psi_k(t^*; \tau)$ can be approximated by a constant. The smaller the time interval $[t_1^*, t_2^*]$, the better $\Psi_k(t^*; \tau)$ is approximated by its mean $c = \frac{1}{t_2^* - t_1^*} \int_{t_1^*}^{t_2^*} \Psi_k(t^*; \tau) dt^*$. By dividing an experiment in small time intervals, in which the data is fitted by the tanh-formula (8), and by “continuously gluing” the intervals that determine y_0 , a set $\{\tau\mu_{N-k}, c\}$ for each interval is obtained. Theory prescribes that all $\tau\mu_{N-k}$ over the intervals should hardly differ, which can serve as an accuracy indication or a verification that the epidemic process is Markovian SIS-like. The set of c values then approximates the non-constant remainder $\Psi_k(t^*; \tau)$, that depends on both the epidemic process and the underlying graph.

Finally, just as higher order mean-field methods can increase the accuracy, our spectral approach can be improved. Instead of bounding the remainder $\Psi_k(t^*; \tau)$ by a constant, which is the zero-order approximation in the Taylor expansion of $\Psi_k(t^*; \tau)$, a polynomial in the prevalence y seems promising [36], which suggests that the method may be refined further. Thus, we believe that it is worthwhile to research $\Psi_k(t^*; \tau)$ in depth to find sharper approximations. Another extension towards more realistic

[45], non-Poissonian infection and curing processes stands on the agenda for further research.

In summary, besides the powerful mean-field approximations, we have demonstrated the potential of a spectral method for the prevalence to unravel properties of SIS (SIR) epidemics on networks.

Acknowledgement. We are grateful to Qiang Liu for the simulations that led to Fig. 3 and Fig. 4.

References

- [1] R. Pastor-Satorras, C. Castellano, P. Van Mieghem, and A. Vespignani. Epidemic processes in complex networks. *Review of Modern Physics*, 87(3):925–979, September 2015.
- [2] J. P. Gleeson, K. P. O’Sullivan, R. A. Baños, and Y. Moreno. Effects of network structure, competition and memory time on social spreading phenomena. *Physical Review X*, 6:021019, 2016.
- [3] R. Pastor-Satorras and A. Vespignani. Epidemic dynamics and endemic states in complex networks. *Physical Review E*, 63:066117, 2001.
- [4] D. J. Watts. *Small Worlds, The Dynamics of Networks between Order and Randomness*. Princeton University Press, Princeton, New Jersey, 1999.
- [5] S. N. Dorogovtsev and J. F. F. Mendes. *Evolution of Networks, From Biological Nets to the Internet and WWW*. Oxford University Press, Oxford, 2003.
- [6] A. Barrat, M. Barthelemy, and A. Vespignani. *Dynamical Processes on Complex Networks*. Cambridge University Press, Cambridge, U.K., 2008.
- [7] M. E. J. Newman. *Networks: An Introduction*. Oxford University Press, Oxford, U. K., 2010.
- [8] P. Van Mieghem. *Performance Analysis of Complex Networks and Systems*. Cambridge University Press, Cambridge, U.K., 2014.
- [9] A. L. Barabási. *Network Science*. Cambridge University Press, Cambridge, U.K., 2016.
- [10] P. Van Mieghem and R. van de Bovenkamp. Accuracy criterion for the mean-field approximation in SIS epidemics on networks. *Physical Review E*, 91(3):032812, March 2015.
- [11] L. Onsager. Crystal statistics: A two-dimensional model with an order-disorder transition. *Physical Review*, 65(3 and 4):117–149, February 1944.
- [12] S. H. Strogatz. From Kuramoto to Crawford: exploring the onset of synchronization in populations of coupled oscillators. *Physica D*, 143:1–20, 2000.
- [13] S. Wolfram. *A New Kind of Science*. Wolfram Media, Inc., 2002.
- [14] P. Bak, C. Tang, and K. Wiesenfeld. Self-organized criticality: An explanation of $1/f$ noise. *Physical Review Letters*, 59(4):381–384, July 1987.
- [15] K.-I. Goh, D.-S. Lee, B. Kahng, and D. Kim. Sandpile on scale-free networks. *Physical Review Letters*, 91(4):148701, October 2003.
- [16] T. Kleiberg and P. Van Mieghem. Self-organization of Internet paths. *IFIP Fourth International Workshop on Self-Organizing Systems, December 9-11, ETH Zurich, Switzerland*, 2009.
- [17] C. Castellano, S. Fortunato, and V. Loreto. Statistical physics of social dynamics. *Reviews of Modern Physics*, 81:591–646, April-June 2009.
- [18] Q. Li, L. A. Braunstein, H. Wang, J. Shao, H. E. Stanley, and S. Havlin. Non-consensus opinion models on complex networks. *Journal of Statistical Physics*, 151(1-2):92–112, 2013.
- [19] H. E. Stanley. *Introduction to Phase Transitions and Critical Phenomena*. Oxford University Press, July 1987.
- [20] N. T. J. Bailey. *The Mathematical Theory of Infectious Diseases and its Applications*. Charlin Griffin & Company, London, 2nd edition, 1975.

- [21] R. M. Anderson and R. M. May. *Infectious Diseases of Humans: Dynamics and Control*. Oxford University Press, Oxford, U.K., 1991.
- [22] D. J. Daley and J. Gani. *Epidemic modelling: An Introduction*. Cambridge University Press, Cambridge, U.K., 1999.
- [23] O. Diekmann, H. Heesterbeek, and T. Britton. *Mathematical Tools for Understanding Infectious Disease Dynamics*. Princeton University Press, Princeton, USA, 2012.
- [24] I. Z Kiss, J. C. Miller, and P. L Simon. *Mathematics of network epidemics: from exact to approximate models*. Springer, 2016.
- [25] P. Van Mieghem and R. van de Bovenkamp. Non-Markovian infection spread dramatically alters the SIS epidemic threshold in networks. *Physical Review Letters*, 110(10):108701, March 2013.
- [26] E. Cator, R. van de Bovenkamp, and P. Van Mieghem. Susceptible-Infected-Susceptible epidemics on networks with general infection and curing times. *Physical Review E*, 87(6):062816, June 2013.
- [27] E. Cator and P. Van Mieghem. Second order mean-field SIS epidemic threshold. *Physical Review E*, 85(5):056111, May 2012.
- [28] P. Holme and J. Saramäki. Temporal networks. *Physics Reports*, 519:97–125, 2012.
- [29] P. Van Mieghem. Approximate formula and bounds for the time-varying SIS prevalence in networks. *Physical Review E*, 93(5):052312, 2016.
- [30] P. Van Mieghem, F. D. Sahneh, and C. Scoglio. Exact Markovian SIR and SIS epidemics on networks and an upper bound for the epidemic threshold. *Proceedings of the 53rd IEEE Conference on Decision and Control (CDC2014), December 15-17, Los Angeles, CA, USA*, 2014.
- [31] D. Brockmann and D. Helbing. The hidden geometry of complex, network-driven contagion phenomena. *Science*, 342:1337–1342, December 2013.
- [32] P. Van Mieghem. *Graph Spectra for Complex Networks*. Cambridge University Press, Cambridge, U.K., 2011.
- [33] A. Ganesh, L. Massoulié, and D. Towsley. The effect of network topology on the spread of epidemics. *IEEE INFOCOM2005*, 2005.
- [34] K. Drakopoulos, A. Ozdaglar, and J. N. Tsitsiklis. A lower bound on the performance of dynamic curing policies for epidemics on graphs. *Proceedings of the 54th IEEE Conference on Decision and Control, December, Osaka, Japan*, 2015.
- [35] M. Fiedler. Algebraic connectivity of graphs. *Czechoslovak Mathematical Journal*, 23(2):298–305, 1973.
- [36] Q. Liu and P. Van Mieghem. Evaluation of an analytic, approximate formula for the time-varying SIS prevalence in different networks. in preparation 2016.
- [37] P. Van Mieghem. The N - Intertwined SIS epidemic network model. *Computing*, 93(2):147–169, 2011.
- [38] W. O. Kermack and A. G. McKendrick. A contribution to the mathematical theory of epidemics. *Proceedings of the Royal Society London, A*, 115:700–721, February 1927.
- [39] E. Cator and P. Van Mieghem. Susceptible-Infected-Susceptible epidemics on the complete graph and the star graph: Exact analysis. *Physical Review E*, 87(1):012811, January 2013.
- [40] M. Draief and L. Massoulié. *Epidemics and Rumours in Complex Networks*. London Mathematical Society Lecture Node Series: 369. Cambridge University Press, Cambridge, UK, 2010.
- [41] R. van de Bovenkamp and P. Van Mieghem. Survival time of the susceptible-infected-susceptible infection process on a graph. *Physical Review E*, 92:032806, 2015.
- [42] P. Van Mieghem. Decay towards the overall-healthy state in SIS epidemics on networks. *arXiv:1310.3980*, 2013.
- [43] S. Trajanovski, J. Martin-Hernandez, W. Winterbach, and P. Van Mieghem. Robustness envelopes of networks. *Journal of Complex Networks*, 1:44–62, 2013.
- [44] Q. Liu and P. Van Mieghem. Die-out probability in SIS epidemic processes on networks. *Fifth International Workshop on Complex Networks and their Applications, 30 November - 2 December, Milan, Italy*, 2016.

- [45] C. Doerr, N. Blenn, and P. Van Mieghem. Lognormal infection times of online information spread. *PLoS ONE*, 8(5):e64349, May 2013.
- [46] P. Van Mieghem. Graph eigenvectors, fundamental weights and centrality metrics for nodes in networks. Delft University of Technology, Report20150808 (www.nas.ewi.tudelft.nl/people/Piet/TUDELFTReports); *arXiv:1401.4580*, 2015.
- [47] S. Barik, S. Fallat, and S. Kirkland. On Hadamard diagonalizable graphs. *Linear Algebra and its Applications*, 435:1885–1902, 2011.
- [48] P. Van Mieghem and E. Cator. Epidemics in networks with nodal self-infections and the epidemic threshold. *Physical Review E*, 86(1):016116, July 2012.

A The basic differential equation of the SIS prevalence

Theorem 1 Let $\tilde{Q}(t) = \tilde{\Delta}(t) - \tilde{A}(t)$ denote the time-dependent, weighted Laplacian, which is an $N \times N$ positive semi-definite symmetric matrix, with the diagonal matrix $\tilde{\Delta}(t) = \text{diag}(\tilde{d}_1, \tilde{d}_2, \dots, \tilde{d}_N)$ and the infection strength of node k is $\tilde{d}_k = \sum_{i=1}^N \beta_{ki} a_{ki}$. If the link infection rate is the same in both directions, $\beta_{ki} = \beta_{ik}$, then the corresponding heterogeneous SIS prevalence differential equation is

$$N \frac{dy(t)}{dt} = -E \left[\tilde{\delta}^T w(t) \right] + E \left[(w(t))^T \tilde{Q}(t) w(t) \right]$$

If the link infection rate is not the same in both directions, $\beta_{ki} \neq \beta_{ik}$, a Laplacian representation is not possible and we end up with

$$N \frac{dy(t)}{dt} = -E \left[\tilde{\delta}^T w(t) \right] + E \left[(u - w(t))^T \tilde{A} w(t) \right]$$

In a homogeneous SIS epidemic process, where all $\beta_{ij} = \beta$ and $\delta_j = \delta$, then (4) simplifies to the differential equation,

$$\frac{dy(t^*; \tau)}{dt^*} = -y(t^*; \tau) + \frac{\tau}{N} E \left[w(t^*; \tau)^T Q w(t^*; \tau) \right]$$

Proof: Summing the Markovian heterogeneous SIS governing equation (3) for the infection probability of node i over all nodes and omitting the time-dependence in $X_i(t)$ to shorten the equations, yields

$$\frac{dE \left[\sum_{i=1}^N X_i \right]}{dt} = E \left[- \sum_{i=1}^N \delta_i X_i + \sum_{k=1}^N \sum_{i=1}^N \beta_{ki} a_{ki} X_k - \sum_{k=1}^N \sum_{i=1}^N \beta_{ki} a_{ki} X_i X_k \right]$$

After rewriting in matrix notation and in terms of the prevalence (2), we obtain

$$\begin{aligned} N \frac{dy(t; \tau)}{dt} &= -E \left[\tilde{\delta}^T w(t) \right] + E \left[\left(\tilde{A} u \right)^T w(t) - w(t)^T \tilde{A} w(t) \right] \\ &= -E \left[\tilde{\delta}^T w(t) \right] + E \left[(u - w(t))^T \tilde{A} w(t) \right] \end{aligned}$$

We define the weighted Laplacian as $\tilde{Q} = \tilde{\Delta} - \tilde{A}$, where the diagonal matrix $\tilde{\Delta} = \text{diag}(\tilde{d}_1, \tilde{d}_2, \dots, \tilde{d}_N)$ and the strength of node k is $d_k = \sum_{i=1}^N \beta_{ki} a_{ki}$. In order to benefit from the basic Laplacian property $\tilde{Q}u = 0$ of a constant row and column sum, we confine ourselves to a symmetric weighted adjacency matrix $\tilde{A} = \left(\tilde{A} \right)^T$, implying that $\beta_{ij} = \beta_{ji}$. Thus, the infection rate of a link is only link dependent and the same in both directions: from node i to node j and vice versa. Consequently, the weighted Laplacian is symmetric, $\tilde{Q} = \left(\tilde{Q} \right)^T$. Under this symmetry restriction, we have

$$\begin{aligned} (u - w(t))^T \tilde{A} w(t) &= (u - w(t))^T \left(\tilde{\Delta} - \tilde{Q} \right) w(t) \\ &= (u - w(t))^T \tilde{\Delta} w(t) - u^T \tilde{Q} w(t) + (w(t))^T \tilde{Q} w(t) \\ &= (w(t))^T \tilde{Q} w(t) \end{aligned}$$

because

$$(u - w(t))^T \tilde{\Delta} w(t) = \sum_{j=1}^N (1 - X_j(t)) X_j(t) \tilde{d}_j = 0$$

since $(1 - X_j(t)) X_j(t) = 0$ as $X_j(t) \in \{0, 1\}$. The homogeneous case (5), as discussed in [29], follows directly from (4) with normalized time $t^* = t\delta$. \square

Perhaps surprising, the exact governing equations (4) and (5) of the SIS prevalence are formally easier than their mean-field counterpart (see [8, p. 467]).

By using the basic definition $Q = BB^T$ of the $N \times N$ Laplacian [32, p. 14] in terms of the $N \times L$ incidence matrix B , we directly find [32, p. 72] that, for any $N \times 1$ vector z ,

$$z^T Q z = (B^T z)^T B^T z = \sum_{l \in \mathcal{L}} (z_{l^+} - z_{l^-})^2$$

where each link l joins two end nodes l^+ and l^- . In particular, for $z = w$, we observe that

$$w^T Q w = \sum_{l \in \mathcal{L}} (X_{l^+} - X_{l^-})^2 \quad (11)$$

If both end of a link l are either infected or healthy, then $X_{l^+} - X_{l^-} = 0$ and such a link l does not contribute to the sum. Hence, only links with one end infected and the other end healthy, for which $(X_{l^+} - X_{l^-})^2 = 1$, contribute precisely a unit amount to $w^T Q w$. In other words, $w^T Q w$ equals the number of links in the cut-set.

B Kernel of the Laplacian Q of a graph with k disconnected components

A graph G has k components (or clusters) if there exists a relabeling of the nodes such that the adjacency matrix has the structure

$$A = \begin{bmatrix} A_1 & O & \dots & O \\ O & A_2 & & \vdots \\ \vdots & & \ddots & \\ O & & \dots & A_k \end{bmatrix}$$

where the square submatrix A_m is the $n_m \times n_m$ adjacency matrix of the connected component m containing n_m nodes. The total number of nodes in G equals $N = \sum_{m=1}^k n_m$. The corresponding Laplacian is

$$Q = \begin{bmatrix} Q_1 & O & \dots & O \\ O & Q_2 & & \vdots \\ \vdots & & \ddots & \\ O & & \dots & Q_k \end{bmatrix}$$

Since $Q_m u_{n_m} = 0$ for each connected component m and the (unscaled) $n_m \times 1$ all-one eigenvector u_{n_m} is the only eigenvector belonging to eigenvalue $\mu_{n_m} = 0$ (due to the connectivity of the connected component m), we find that the general representation of an eigenvector $x_N(m)$ of Q belonging to the eigenvalue $\mu_N = 0$ with multiplicity k is

$$x_N^T(m) = (\eta_{m1} u_{n_1}^T, \eta_{m2} u_{n_2}^T, \dots, \eta_{mk} u_{n_k}^T) \quad (12)$$

The subspace of the N -dimensional space spanned by the eigenvectors of a matrix belonging to the zero eigenvalue is called the kernel or null space of that matrix. Each of the k possible $N \times 1$ eigenvectors $x_N(m)$ of Q have the form (12) and can thus be specified by a $k \times 1$ vector $\eta_m = (\eta_{m1}, \eta_{m2}, \dots, \eta_{mk})$ for $1 \leq m \leq k$. Any pair $\{x_N(m), x_N(s)\}$ of such (normalized) eigenvectors, represented by the vectors $\eta_m = (\eta_{m1}, \eta_{m2}, \dots, \eta_{mk})$ and $\eta_s = (\eta_{s1}, \eta_{s2}, \dots, \eta_{sk})$, must be orthogonal [32], which leads to the set of $\binom{k}{2}$ non-linear equations

$$x_N(m) x_N^T(s) = \sum_{j=1}^k \eta_{mj} \eta_{sj} n_j = \delta_{ms}$$

Let us define the vector $y_m = (y_{m1}, y_{m2}, \dots, y_{mk})$ with $y_{mj} = \sqrt{n_j} \eta_{mj}$, then the above orthogonality condition reduces to the “ordinary” orthogonality condition for the set of k vectors y_1, y_2, \dots, y_k ,

$$y_m^T y_s = \sum_{j=1}^k y_{mj} y_{sj} = \delta_{ms}$$

This means that any set of k orthogonal vectors y_1, y_2, \dots, y_k , that spans the k -dimensional space, can be used to produce k eigenvectors $x_N(m)$, with $1 \leq m \leq k$, of the kernel of Q . The corresponding $k \times k$ matrix Y_k , with the vectors y_1, y_2, \dots, y_k in the columns, is an orthogonal matrix, whose properties with respect to graphs are studied in [46]. Clearly, the simplest set is the set e_1, e_2, \dots, e_k of the basis vectors for which $Y_k = I$. Since any other $N \times 1$ eigenvectors of Q belonging to a positive eigenvalue of Q is orthogonal to each kernel eigenvector $x_N(m)$ that belongs to the zero eigenvalue $\mu_N = 0$, we observe that there exist a k -fold infinity of such eigenvector sets, depending on our choice of the set of k vectors y_1, y_2, \dots, y_k .

Since the Bernoulli vector w has only zero and one components, the scalar product $w^T x_N(m)$ is maximized if one the vectors y_m is equal to the $k \times 1$ all-one vector u_k . This observation suggests us to construct the set of orthogonal eigenvectors y_1, y_2, \dots, y_k , with one of them, say $y_1 = u_k$, equal to the all-one vector u_k . Basically, this means that all orthogonal vectors y_1, y_2, \dots, y_k are eigenvectors of the adjacency matrix of the complete graph K_k , because the unscaled largest adjacency eigenvector (of any regular graph and thus also of K_k) is $x_1(K_k) = u_k$.

Barik *et al.* [47] have shown that only regular graphs, such as the complete graph K_N , for $N = 4k$ and $k \in \mathbb{N}_0$, and the regular bipartite graph $K_{2k,2k}$, are diagonalizable by a symmetric Hadamard matrix. An $n \times n$ Hadamard matrix H_n contains as elements either -1 and 1 and obeys $H_n H_n^T = nI_n$. The normalized matrix $\frac{1}{\sqrt{n}} H_n$ is an orthogonal matrix, from which it follows that $\det H_n = n^{\frac{n}{2}}$, which is maximal among all $n \times n$ matrices with elements in absolute value less than or equal to 1, which includes all orthogonal matrices. Indeed, let $H_n = [u | \tilde{H}]$ so that $H_n e_1 = u_n$. Consider the diagonal matrix $D = I - e_1 e_1^T$, then

$$H_n D H_n^T = H_n H_n^T - H_n e_1 (H_n e_1)^T = nI_n - u_n u_n^T = nI - J$$

Hence, the Laplacian matrix of the complete graph K_n is $Q_{K_n} = nI - J = H_n D H_n^T$. Since K_n is a regular graph, the eigenvectors of the Laplacian Q and the adjacency matrix A are the same [32]. In conclusion, any Hadamard matrix with first column $H_n e_1 = u_n$ provides the orthogonal eigenvector matrix for the complete graph K_n .

In summary, by choosing an $k \times k$ normalized Hadamard matrix $Y_k = \frac{1}{\sqrt{k}}H_k$ with first column $H_k e_1 = u_k$, all components $\eta_{mj} = \frac{y_{mj}}{\sqrt{n_j}}$ in (12) are determined, leading, with $(\Upsilon_k)_{mj} = \eta_{mj}$, to the matrix $\Upsilon_k = \text{diag}\left(\frac{1}{\sqrt{n_j}}\right) Y_k = \frac{1}{\sqrt{k}} \text{diag}\left(\frac{1}{\sqrt{n_j}}\right) H_k$. Moreover, the scalar product $w^T \xi$ is maximal among all normalized vectors ξ for $\xi = x_N(1)$; in particular, $w^T x_N(1) = \frac{w^T u}{\sqrt{N}} = \frac{w^T w}{\sqrt{N}}$.

C The quadratic form $z^T Q z$ in a graph with k disconnected components and its spectral decomposition

C.1 The vector z is real

Since the eigenvectors of Q constitute an orthogonal basis, any $N \times 1$ real vector z can be expressed as a linear combination of eigenvectors x_1, x_2, \dots, x_N of Q ,

$$z = \sum_{j=1}^N \alpha_j x_j$$

where $\alpha_j = z^T x_j$ and x_j is the eigenvector belonging to the j -th largest Laplacian eigenvalue μ_j . In terms of the orthogonal matrix X with eigenvector in its columns [46], which satisfies the orthogonality conditions $XX^T = X^T X = I$ so that $X^{-1} = X^T$, we have

$$\alpha = X^T z \text{ and } z = X \alpha$$

illustrating the one-to-one relation between the coordinates of z expressed in a certain basis and its coordinates α expressed in the basis of eigenvectors of Q . The quadratic form equals

$$z^T Q z = \sum_{k=1}^N \sum_{m=1}^N \alpha_k \alpha_m x_k^T Q x_m = \sum_{k=1}^N \alpha_k^2 \mu_k \quad (13)$$

When the graph G is disconnected into k connected components (Appendix B), there holds [32, p. 74] that $\mu_{N-j} = 0$ for $0 \leq j \leq k-1$. In other words, the k smallest eigenvalues of the Laplacian Q are zero, whereas all the others are positive $\mu_1 \geq \mu_2 \geq \dots \geq \mu_{N-k} > 0$. Thus,

$$z^T z = \sum_{j=1}^N \alpha_j^2 = \sum_{j=1}^{N-k} \alpha_j^2 + \sum_{j=N-k+1}^N \alpha_j^2$$

Further, as shown in (12) above for $k > N - m$ and writing z as a k -block vector,

$$z^T = (\hat{z}_1^T, \hat{z}_2^T, \dots, \hat{z}_k^T)$$

where \hat{z}_j is an $n_j \times 1$ vector corresponding to the block structure of the connected components in the adjacency matrix, the projection of the vector z onto the kernel vectors $x_N(m)$ for $1 \leq m \leq k$ of the Laplacian Q is

$$z^T x_N(m) = \sum_{j=1}^k \eta_{mj} \left(u_{n_j}^T \hat{z}_j \right)$$

so that

$$\sum_{j=N-k+1}^N \alpha_j^2 = \sum_{m=1}^k \left(\sum_{j=1}^k \eta_{mj} \left(u_{n_j}^T \widehat{z}_j \right) \right)^2$$

In conclusion, for a graph G with k connected components, the Euclidean norm of the vector z can be written as

$$z^T z = \frac{1}{N} (u^T z)^2 + \sum_{m=2}^k \left(\sum_{j=1}^k \eta_{mj} \left(u_{n_j}^T \widehat{z}_j \right) \right)^2 + \sum_{j=1}^{N-k} \alpha_j^2 \quad (14)$$

where each element η_{mj} of the matrix $\Upsilon_k = \frac{1}{\sqrt{k}} \text{diag} \left(\frac{1}{\sqrt{n_j}} \right) H_k$ can be determined, as shown in Appendix B.

C.2 The Bernoulli random vector w is a binary vector

The Bernoulli vector w is a so-called binary vector, because each component $w_k = X_k$ is either zero or one. For such vectors, we observe with (1) that

$$w^T w = \sum_{k=1}^N X_k^2 = \sum_{k=1}^N X_k = u^T w = NS$$

Let us consider the eigenvector decomposition

$$w = \sum_{j=1}^N \zeta_j x_j \quad (15)$$

where $\zeta_j = w^T x_j$ is the j -th coordinate of the Bernoulli vector w along the j -th eigenvector x_j in the eigenspace of Q . For a graph G with k connected components, (14) leads to

$$w^T w = \frac{1}{N} (u^T w)^2 + \sum_{m=2}^k \left(\sum_{j=1}^k \eta_{mj} \left(u_{n_j}^T w_j \right) \right)^2 + \sum_{j=1}^{N-k} \zeta_j^2$$

or, with $w^T w = u^T w = NS$,

$$\sum_{j=1}^{N-k} \zeta_j^2 = N (S - S^2) - \sum_{m=2}^k \left(\sum_{j=1}^k \eta_{mj} \left(u_{n_j}^T w_j \right) \right)^2 \quad (16)$$

Next, since $\mu_{N-j} = 0$ for $0 \leq j \leq k-1$, the quadratic form (13) becomes

$$w^T Q w = \sum_{j=1}^{N-k} \zeta_j^2 \mu_j \quad (17)$$

Introducing the square of the coordinate, obtained from (16),

$$\zeta_{N-k}^2 = N (S - S^2) - \sum_{m=2}^k \left(\sum_{j=1}^k \eta_{mj} \left(u_{n_j}^T w_j \right) \right)^2 - \sum_{j=1}^{N-k-1} \zeta_j^2$$

into (17) yields

$$\begin{aligned}
w^T Q w &= \zeta_{N-k}^2 \mu_{N-k} + \sum_{j=1}^{N-k-1} \zeta_j^2 \mu_j \\
&= \mu_{N-k} N (S - S^2) - \mu_{N-k} \sum_{m=2}^k \left(\sum_{j=1}^k \eta_{mj} (u_{n_j}^T w_j) \right)^2 - \sum_{j=1}^{N-k-1} \mu_{N-k} \zeta_j^2 + \sum_{j=1}^{N-k-1} \zeta_j^2 \mu_j
\end{aligned}$$

Rewritten,

$$w^T Q w = \mu_{N-k} N (S - S^2) + R_k \quad (18)$$

where the correction R_k is

$$R_k = \sum_{j=1}^{N-k-1} \zeta_j^2 (\mu_j - \mu_{N-k}) - \mu_{N-k} \sum_{m=2}^k \left(\sum_{j=1}^k \eta_{mj} (u_{n_j}^T \hat{w}_j) \right)^2 \quad (19)$$

where \hat{w}_j here is the j -th $n_j \times 1$ block vector of w according to the component structure of the graph G . Thus, $u_{n_j}^T \hat{w}_j$ equals the number of infected nodes at time t in the j -th connected component of G with n_j nodes and, with $N = \sum_{m=1}^k n_m$, the fraction S of infected nodes in G (at time t) is a “weighted” average over the k components of G

$$S = \frac{\sum_{j=1}^k u_{n_j}^T \hat{w}_j}{\sum_{m=1}^k n_m}$$

The first term in R_k is non-negative, as well as the second term. In a connected graph G where $k = 1$, the second term in (19) vanishes so that R_1 is non-negative, but only zero for the complete graph K_N . When $k = 1$, the general expression R_k in (19) reduces to our previous expression in [29] in terms of the algebraic connectivity μ_{N-1} . Clearly, the second term in (19) only appears when a graph is disconnected into k connected components. When k is large, then R_k is likely negative, and certainly for $k = N - 1$, in which case the first in (19) term vanishes.

For a given graph G , all parameters related its Laplacian eigenstructure, such as the eigenvalues μ_j and the elements η_{mj} of the Hadamard related matrix $\Upsilon_k = \frac{1}{\sqrt{k}} \text{diag}\left(\frac{1}{\sqrt{n_j}}\right) H_k$, are known. Only the coordinates ζ_j for $1 \leq j \leq N - k$ and kernel coordinates $u_{n_j}^T \hat{w}_j$ for $1 \leq j \leq k$ in (19) depend on the SIS process via the Bernoulli vector $w(t)$, that depends upon its initial value at $w(0)$ at time $t = 0$. Indeed, if the initially infected nodes only appear in one component, say $m = 1$, so that the vector $\hat{w}_1(0) \neq 0$, then all other vectors $\hat{w}_m = 0$ for all components $m > 1$, because evidently, an infection can only spread in a connected component.

C.3 A Fourier analysis interpretation of Laplacian eigenvectors

If x_k is an eigenvector of Q belonging to eigenvalue μ_k , then the fundamental Laplacian quadratic form in (11) becomes

$$\mu_k = x_k Q x_k = \sum_{l \in \mathcal{L}} ((x_k)_{l+} - (x_k)_{l-})^2$$

which implies that the variation of eigenvector components at both ends of a link increases with the Laplacian eigenvalue. When interpreting the eigenvector x_k as a function $(x_k)_i$ of the nodal components

i at frequency μ_k , the above suggests that a high frequency Laplacian eigenvector oscillates more (over a link) than a low frequency Laplacian eigenvector. The suggestion is correct for a ring graph [32, p. 116-123], because the orthogonal eigenvector matrix X of the ring graph is the Fourier matrix (with the usual cosine and sine as eigenfunctions). While a general theorem valid for any graph that the Laplacian eigenvector x_k possesses more sign changes with increasing μ_k – a reflection of higher oscillatory behavior with increasing frequency – seems missing¹, the intuition of the Fourier decomposition of a signal hints that the “Fourier coefficients” $\zeta_k = w^T x_k$ are generally expected to decrease with higher index k . If correct and if $\zeta_k^2 \mu_k$ decreases generally with μ_k , then the first sum of R_k in (19) would generally consists of decreasing positive terms. This interpretation may lead to sharp approximations of R_k .

D Governing equation of the homogeneous SIS prevalence in graph with k disconnected components

Invoking the definition (2) of the prevalence $y = E[S]$, $E[S - S^2] = y - E[S^2]$ and $E[S^2] = y^2 + \text{Var}[S]$, (18) becomes

$$\begin{aligned} \frac{1}{N} E[w^T Q w] &= \mu_{N-k} E[S] - \mu_{N-k} E[S^2] + \frac{E[R_k]}{N} \\ &= \mu_{N-k} y - \mu_{N-k} y^2 - \mu_{N-k} \left(\text{Var}[S] - \frac{E[R_k]}{N \mu_{N-k}} \right) \end{aligned} \quad (20)$$

Using (5), the spectral representation of the SIS prevalence governing differential equation is

$$\frac{dy(t^*; \tau)}{dt^*} = (\tau \mu_{N-k} - 1) y(t^*; \tau) - \tau \mu_{N-k} y^2(t^*; \tau) - \Psi_k(t^*; \tau)$$

where the remainder

$$\Psi_k(t^*; \tau) = \tau \mu_{N-k} \left(\text{Var}[S(t^*; \tau)] - \frac{E[R_k(t^*; \tau)]}{N \mu_{N-k}} \right)$$

For a connected graph (i.e. with $k = 1$ connected component), we again find the earlier result in [29, eq. (12)]. Introducing (19), the explicit form of the remainder is

$$\frac{\Psi_k(t^*; \tau)}{\tau \mu_{N-k}} = \text{Var}[S(t^*; \tau)] + \frac{1}{N} \sum_{m=2}^k E \left[\left(\sum_{j=1}^k \eta_{mj} (u_{n_j}^T w_j) \right)^2 \right] - \frac{1}{N} \sum_{j=1}^{N-k-1} \left(\frac{\mu_j}{\mu_{N-k}} - 1 \right) E[\zeta_j^2] \quad (21)$$

illustrating that $\Psi_k(t^*; \tau)$ is likely positive for large k , i.e. in a graph with many connected components.

For small time, the Taylor expansion yields

$$y(t^* | \tau) = y(0 | \tau) + \left. \frac{dy(t^*; \tau)}{dt^*} \right|_{t^*=0} t^* + O(t^{*2})$$

Invoking the differential equation (7) and $y(0 | \tau) = y_0$ leads to

$$y(t^* | \tau) = y_0 + \{y_0 (\tau \mu_{N-k} - 1) - y_0^2 \tau \mu_{N-k} - \Psi_k(0; \tau)\} t^* + O(t^{*2})$$

¹Any symmetric matrix can be reduced by orthogonal Householder reflections to a tri-band matrix, whose eigenvector structure consists of orthogonal polynomials and is computed in [8, p. 565-573],[42].

where $\Psi_1(0; \tau)$ is small (because $\text{Var}[S(0; \tau)] = 0$ since $S(0)$ is deterministic). The tanh-approximation (8), on the other hand, replaces $\Psi_k(t^*; \tau)$ by c (in any time interval) so that

$$T(t^*|y_0, \tau\mu_{N-k}, c) = y_0 + y_0 \left\{ \tau\mu_{N-k}(1 - y_0) - \left(1 + \frac{c}{y_0}\right) \right\} t^* + O(t^{*2})$$

The initial slope is non-negative when $\tau \geq \frac{1}{\mu_{N-k}} \left(\frac{1 + \frac{c}{y_0}}{1 - y_0} \right)$. For a connected graph ($k = 1$), the tanh-prevalence $T(t^*|y_0, \tau\mu_{N-1}, c)$ increases for $\tau > \tau_c$ for all time $t^* \geq 0$ and, hence,

$$\frac{1}{\mu_{N-1}} \left(\frac{1 + \frac{c}{y_0}}{1 - y_0} \right) > \tau_c$$

or

$$c > y_0 \tau_c \mu_{N-1} (1 - y_0) - y_0 \geq y_0 \frac{\mu_{N-1}}{\lambda_1} (1 - y_0) - y_0$$

because the lower bound for the epidemic threshold obeys $\tau_c \geq \frac{1}{\lambda_1}$ (see e.g. [1, 29]). Since $\mu_{N-1} < \lambda_1$ (except for the complete graph and regular multipartite graphs), the positive-slope condition would suggest that $c \gtrsim -y_0$ for almost all graphs. The value $c \approx -y_0$ is also approximately deduced from the Kermack and McKendrick [38] analysis for SIR. Simulations [36] seem to agree roughly with $c \approx -y_0$.

For large time, the tanh-formula (8) reduces to

$$\lim_{t^* \rightarrow \infty} T(t^*|y_0, \tau\mu_{N-k}, c) = \frac{1}{2} \left(1 - \frac{1}{\tau\mu_{N-k}} \right) + \frac{1}{2} \sqrt{\left(1 - \frac{1}{\tau\mu_{N-k}} \right)^2 - \frac{4c}{\tau\mu_{N-k}}} \quad (22)$$

which corresponds to the metastable state of the SIS process. For some extremal values of c , (22) shows that

$$\begin{aligned} \lim_{t^* \rightarrow \infty} T(t^*|y_0, \tau\mu_{N-k}, -1) &= 1 \\ \lim_{t^* \rightarrow \infty} T(t^*|y_0, \tau\mu_{N-k}, 0) &= \begin{cases} 1 - \frac{1}{\tau\mu_{N-k}} & \tau > \frac{1}{\mu_{N-k}} \\ 0 & \tau < \frac{1}{\mu_{N-k}} \end{cases} \end{aligned}$$

For $c_{\text{real}} = \frac{\tau\mu_{N-k}}{4} \left(1 - \frac{1}{\tau\mu_{N-k}} \right)^2 \geq 0$, that guarantees a real prevalence ($\Xi = 0$ in (10)), the prevalence does not depend on time any more and $T(t^*|y_0, \tau\mu_{N-k}, c_{\text{real}}) = \frac{1}{2} \left(1 - \frac{1}{\tau\mu_{N-k}} \right)$. Moreover, for $\tau < \frac{1}{\mu_{N-k}}$, positive $c > 0$ are not physical since the prevalence can become negative. For $\tau > \frac{1}{\mu_{N-k}}$, a positive $c < c_{\text{real}}$ can be possible.

Similarly to [29] for the case $k = 1$ of a connected graph, $T(t^*|y_0, s, c)$ in (8) obeys the Riccati differential equation

$$\frac{dT}{dt^*} = (s - 1)T - sT^2 - c$$

For the same initial prevalence $y(0) = \tilde{y}_k(0) = y_0$ and given the constants $c_L(k)$ and $c_H(k)$, that satisfy $c_L(k) \leq \Psi_k(t^*; \tau) \leq c_U(k)$, the prevalence $y(t^*)$ at normalized time t^* is bounded by the relatively simple expression (8)

$$\begin{cases} y(t^*) \geq T(t^*|y_0, \tau\mu_{N-k}, c_U(k)) & \text{if } \Psi_k(t^*; \tau) \leq c_U(k) \text{ for } t^* \in [t_1^*, t_2^*] \\ y(t^*) \leq T(t^*|y_0, \tau\mu_{N-k}, c_L(k)) & \text{if } \Psi_k(t^*; \tau) \geq c_L(k) \text{ for } t^* \in [t_1^*, t_2^*] \end{cases}$$

The upper bound $\Psi_k(t^*; \tau) \leq c_U(k)$ implies that $y(t^*) \geq T(t^* | y_0, \tau \mu_{N-k}, c_U(k))$ and $T(t^* | y_0, \tau \mu_{N-k}, c_U(k))$ is real if the discriminant in (10) is positive,

$$\left(1 - \frac{1}{\tau \mu_{N-k}}\right)^2 \geq \frac{4c}{\tau \mu_{N-k}} \geq \frac{4\Psi_k(t^*; \tau)}{\tau \mu_{N-k}} = 4 \left(\text{Var}[S(t^*; \tau)] - \frac{E[R_k(t^*; \tau)]}{N \mu_{N-k}} \right)$$

If $\text{Var}[S(t^*; \tau)] \geq \frac{E[R_k(t^*; \tau)]}{N \mu_{N-k}}$ (i.e. $c_L(k) \geq 0$), then the inequality is equivalent to the lower bound for the effective infection rate

$$\tau \geq \frac{1}{\mu_{N-k} \left(1 - 2\sqrt{\text{Var}[S(t^*; \tau)] - \frac{E[R_k(t^*; \tau)]}{N \mu_{N-k}}}\right)} \geq \frac{1}{\mu_{N-k}} \quad (23)$$

that guarantees to operate in the endemic regime when t^* is sufficiently large. We observe that, the more connected components a graph on N nodes has, the larger k and μ_{N-k} and, consequently, the lower $\frac{1}{\mu_{N-k}}$. Physically, the larger k , the fewer nodes a connected component has (on average k/N) and the larger the epidemic threshold of a connected component should become, because $\tau_c > \tau_c^{(1)} = \frac{1}{\lambda_1}$ increases with decreasing λ_1 and the spectral radius $\lambda_1 \geq E[D]$, which, in dense graphs, increases with N on average. Hence, we expect that the epidemic threshold in a graph with k connected components increases and (23) would imply that $\text{Var}[S(t^*; \tau)] - \frac{E[R_k(t^*; \tau)]}{N \mu_{N-k}} \rightarrow \frac{1}{4}$ for sufficiently large t^* .

In summary, the analysis generalizes the previous derivations in [29] to graphs with k connected components, as e.g. in temporal networks. We can thus conclude that, for any graph G with k connected components with a fixed topology in some non-zero time interval, the prevalence $y(t^*)$ in that time interval can be bounded by the curve $T(t^* | y_0, s, c)$ in (8) with three parameters: (a) the initial condition y_0 or value of the prevalence at the beginning of the time interval, (b) a Laplacian normalized rate $s = \tau \mu_{N-k}$ and (c) a constant c . Implicitly, the computation of the prevalence also assumes that the number N of nodes in the graph G is known. The prevalence is only non-zero when the effective infection rate τ exceeds the epidemic threshold τ_c . Moreover, it is known that $\tau > \tau_c > \tau_c^{(1)}$, where the NIMFA threshold $\tau_c^{(1)} = \frac{1}{\lambda_1}$ and λ_1 is the largest eigenvalue of the adjacency matrix of the graph G . Hence, the adjacency normalized effective infection rate $x = \lambda_1 \tau$ allows us to compare epidemics in different graphs for sufficiently long time: when $x \leq 1$, the epidemic will die out, whereas $x > 1 + \varepsilon$ with ε a correction due to the mean-field approximation, the epidemic will be persistent. However, the correction ε is unknown. On the other hand, (23) tells us that, when the Laplacian normalized rate $s = \tau \mu_{N-k} \geq \xi$, where $\xi = \frac{1}{1 - 2\sqrt{\text{Var}[S(t^*; \tau)] - \frac{E[R_k(t^*; \tau)]}{N \mu_{N-k}}}} > 1$, we are surely in the endemic regime where the prevalence $y(t^*) > 0$ (for a sufficiently large t^*). Unfortunately, computing ξ is difficult, so that determining which effective infection rate τ leads to persistent infections, is complicated.

In conclusion, an accurate determination of the SIS epidemics threshold regime will likely stay on the scientific agenda for future research.

E Governing equation of the heterogeneous SIS prevalence in graph with k disconnected components

The expression (18) is valid for the weighted Laplacian \tilde{Q} with eigenvectors $\tilde{x}_1, \tilde{x}_2, \dots, \tilde{x}_N = u$ belonging to eigenvalues $\tilde{\mu}_1 \geq \tilde{\mu}_2 \geq \dots \geq \tilde{\mu}_N = 0$, respectively and with the scalar product $\tilde{\zeta}_k = w^T \tilde{x}_k$,

since the kernel space of \tilde{Q} is the same as that of the unweighted Laplacian Q . Invoking the definition of the prevalence $y = E[S]$, $E[S - S^2] = y - E[S^2]$ and $E[S^2] = y^2 + \text{Var}[S]$, (18) becomes

$$\frac{1}{N} E[w^T \tilde{Q} w] = \tilde{\mu}_{N-k} y - \tilde{\mu}_{N-k} y^2 - \tilde{\mu}_{N-k} \left(\text{Var}[S] - \frac{E[\tilde{R}_k]}{N \tilde{\mu}_{N-k}} \right)$$

Introduced into (4), which we write as,

$$\begin{aligned} \frac{dy(t; \tau)}{dt} &= -\frac{1}{N} E \left[\left(\delta_{av} u + \tilde{\delta} - \delta_{av} u \right)^T w(t) \right] + \frac{1}{N} E \left[(w(t))^T \tilde{Q} w(t) \right] \\ &= -\delta_{av} y - \frac{1}{N} E \left[\left(\tilde{\delta}^T - \delta_{av} u^T \right) w(t) \right] + \tilde{\mu}_{N-k} y - \tilde{\mu}_{N-k} y^2 - \tilde{\mu}_{N-k} \left(\text{Var}[S] - \frac{E[\tilde{R}_k]}{N \tilde{\mu}_{N-k}} \right) \end{aligned}$$

where $\left(\tilde{\delta}^T - \delta_{av} u^T \right) w(t)$ is now an additional correction due to heterogeneous, node-depending curing rates. Normalizing the time $\tilde{t}^* = \delta_{av} t$ with respect to average curing rate $\delta_{av} = \frac{\tilde{\delta}^T u}{N}$ and realizing that the eigenvalues of the weighted Laplacian are function of the heterogeneous infection rates β_{ij} , we have

$$\frac{dy(\tilde{t}^*; \tau)}{d\tilde{t}^*} = \left(\frac{\tilde{\mu}_{N-k}}{\delta_{av}} - 1 \right) y - \frac{\tilde{\mu}_{N-k}}{\delta_{av}} y^2 - \frac{\tilde{\mu}_{N-k}}{\delta_{av}} \left(\text{Var}[S] - \frac{E[\tilde{R}_k] - E \left[\left(\tilde{\delta}^T - \delta_{av} u^T \right) w(t) \right]}{N \tilde{\mu}_{N-k}} \right)$$

In summary, the spectral representation of the heterogeneous SIS prevalence governing differential equation in a graph with k connected components is

$$\frac{dy(\tilde{t}^*; \tau)}{d\tilde{t}^*} = \left(\frac{\tilde{\mu}_{N-k}}{\delta_{av}} - 1 \right) y - \frac{\tilde{\mu}_{N-k}}{\delta_{av}} y^2 - \tilde{\Psi}_k(\tilde{t}^*; \tau)$$

where the remainder is

$$\tilde{\Psi}_k(\tilde{t}^*; \tau) = \frac{\tilde{\mu}_{N-k}}{\delta_{av}} \left(\text{Var}[S] - \frac{E[\tilde{R}_k] - E \left[\left(\tilde{\delta}^T - \delta_{av} u^T \right) w(t) \right]}{N \tilde{\mu}_{N-k}} \right)$$

Just as in the homogeneous case (Appendix D), we may proceed by a bounding procedure to find that the heterogeneous SIS prevalence also can be bounded by a tanh-expression of the form (8), though with different coefficients and an even more complicated $\tilde{\Psi}_k(\tilde{t}^*; \tau)$.

F Governing equation of the ε -SIS prevalence in graph with k disconnected components

The differential equation for the average fraction of infected nodes y in the ε -SIS process is [8, p. 455]

$$\frac{dy(t^*; \tau)}{dt^*} = \varepsilon^* - (1 + \varepsilon^*) y(t^*; \tau) + \frac{\tau}{N} E[w^T(t^*; \tau) Q w(t^*; \tau)] \quad (24)$$

where ε is the constant self-infection rate for each node [48]. If $\tau = 0$, the differential equation (24) for the ε -SIS prevalence shows that

$$\frac{dy(t^*; 0, \varepsilon^*)}{dt^*} = \varepsilon^* - (1 + \varepsilon^*) y(t^*; 0, \varepsilon^*)$$

with solution

$$y(t^*; 0, \varepsilon^*) = \frac{\varepsilon^*}{1 + \varepsilon^*} + \left(y_0 - \frac{\varepsilon^*}{1 + \varepsilon^*} \right) e^{-(1 + \varepsilon^*)t}$$

As in previous Section D, after using $y = E[S]$, $E[S - S^2] = y - E[S^2]$ and $E[S^2] = y^2 + \text{Var}[S]$ and (18), the differential equation (24) of the ε -SIS prevalence becomes

$$\frac{dy(t^*; \tau, \varepsilon^*)}{dt^*} = (\tau\mu_{N-k} - (1 + \varepsilon^*))y(t^*; \tau, \varepsilon^*) - \tau\mu_{N-k}y^2(t^*; \tau, \varepsilon^*) - \Psi_k(t^*; \tau, \varepsilon^*)$$

where

$$\Psi_k(t^*; \tau, \varepsilon^*) = \tau\mu_{N-k} \left(\text{Var}[S(t^*; \tau)] - \frac{E[R_k(t^*; \tau)]}{N\mu_{N-k}} \right) - \varepsilon^* \quad (25)$$

Again, by bounding $c_L(k; \varepsilon^*) \leq \Psi_k(t^*; \tau, \varepsilon^*) \leq c_U(k; \varepsilon^*)$, a variant of the tanh-formula (8) applies

$$\tilde{T}(t^* | y_0, s, c; \varepsilon^*) = \frac{1}{2} \left(1 - \frac{1 + \varepsilon^*}{s} \right) + \frac{\Upsilon}{2} \tanh \left(\frac{s\Upsilon}{2} t^* + \text{arctanh} \left(\frac{2y_0 - (1 - \frac{1 + \varepsilon^*}{s})}{\Upsilon} \right) \right) \quad (26)$$

where $s = \tau\mu_{N-k}$ and

$$\Upsilon = \sqrt{\left(1 - \frac{1 + \varepsilon^*}{s} \right)^2 - \frac{4c}{s}}$$

which clearly reduces to (26) for $\varepsilon^* = 0$.

F.1 Extremal values of the ε -SIS prevalence

When the prevalence attains an extremum $y(p; \tau, \varepsilon^*)$ at time $t^* = p$, obeying $\left. \frac{dy(t^*; \tau, \varepsilon^*)}{dt^*} \right|_{t^*=p} = 0$, then

$$\tau\mu_{N-k}y^2(p; \tau, \varepsilon^*) - (\tau\mu_{N-k} - (1 + \varepsilon^*))y(p; \tau, \varepsilon^*) + \Psi_k(p; \tau, \varepsilon^*) = 0$$

There are only real solutions for the ‘‘time-extremal’’ prevalence,

$$y_{\pm}(p; \tau, \varepsilon^*) = \frac{(\tau\mu_{N-k} - (1 + \varepsilon^*)) \pm \sqrt{(\tau\mu_{N-k} - (1 + \varepsilon^*))^2 - 4\tau\mu_{N-k}\Psi_k(p; \tau, \varepsilon^*)}}{2\tau\mu_{N-k}}$$

and

$$y_{\pm}(p; \tau, \varepsilon^*) = \left(1 - \frac{1 + \varepsilon^*}{\tau\mu_{N-k}} \right) \frac{1}{2} \left\{ 1 \pm \sqrt{1 - \frac{\frac{\Psi_k(p; \tau, \varepsilon^*)}{\tau\mu_{N-k}}}{1 - \frac{1 + \varepsilon^*}{\tau\mu_{N-k}}}} \right\} \quad (27)$$

provided the discriminant $(\tau\mu_{N-k} - (1 + \varepsilon^*))^2 - 4\tau\mu_{N-k}\Psi_k(p; \tau, \varepsilon^*) \geq 0$, which is equivalent to

$$\frac{1}{4} \left(1 - \frac{1 + \varepsilon^*}{\tau\mu_{N-k}} \right)^2 \geq \frac{\Psi_k(p; \tau, \varepsilon^*)}{\tau\mu_{N-k}} = \text{Var}[S(p; \tau)] - \frac{E[R_k(p; \tau)]}{N\mu_{N-k}} - \frac{\varepsilon^*}{\tau\mu_{N-k}}$$

This inequality leads to a lower bound for the effective infection rate,

$$\tau(\varepsilon^*) \geq \frac{1}{\mu_{N-k}} \frac{1 + \varepsilon^*}{1 - 2\sqrt{\text{Var}[S(p; \tau)] - \frac{E[R_k(p; \tau)]}{N\mu_{N-k}} - \frac{\varepsilon^*}{\tau\mu_{N-k}}}} > \tau(0)$$

For small self-infection rates ε^* , we can demonstrate the last inequality, which implies that the effective infection rate to guarantee an endemic regime lies higher for the ε -SIS model than for the classical

($\varepsilon = 0$) SIS-model, which is consistent with the analysis in [8, p. 457-458]. Although surprising at first glance, we need to realize that the steady state in the $\varepsilon = 0$ SIS-model is the overall healthy state, to which the ε -SIS must converge if $\varepsilon \rightarrow 0$, irrespective of the effective infection rate τ . The existence of an absorbing state implies in a finite graph that the epidemics eventually dies out (i.e. the dynamic process will surely hit the absorbing state in the 2^N large Markov state graph). This peculiar limit $\varepsilon \rightarrow 0$ is further illustrated in [48, Fig. 5 and 6].

F.2 The absorbing state

The “time-extremal” prevalence $y_{\pm}(p; \tau, \varepsilon^*)$ at time $t^* = p$ in (27) can only be zero if (a) the negative sign applies and (b) $\Psi_k(p; \tau, \varepsilon^*) = 0$, in which case $y_-(p; \tau, \varepsilon^*) = 0$ for all effective infection rates τ . However, if $y_{\pm}(p; \tau, \varepsilon^*) = 0$, then $S(p) = 0$, which implies that Bernoulli vector $w(p) = 0$. The definition (25) of the remainder $\Psi_k(p; \tau, \varepsilon^*)$ and the specific expression (19) for the spectral correction R_k illustrate that $\Psi_k(p; \tau, \varepsilon^*) = -\varepsilon^*$ if $S(p) = 0$. Consequently, $y_-(p; \tau, \varepsilon^*) = 0$ and $\Psi_k(p; \tau, \varepsilon^*) = 0$ can only be satisfied if $\varepsilon^* = 0$, thus only in the classical SIS process. This singular condition, $y_-(p; \tau, \varepsilon^*) = 0$ and $\Psi_k(p; \tau, \varepsilon^*) = 0$, which holds irrespective of the effective infection rate τ , corresponds to the absorbing state which is attained at time p . If $\varepsilon^* > 0$, there cannot be an absorbing state and the negative sign solution $y_-(p; \tau, \varepsilon^*)$ in (27), which is decreasing in τ , does not exist. Moreover, Markov theory [8] states the ε -SIS Markovian chain possesses a unique steady-state, which corresponds to $y_+(p; \tau, \varepsilon^*)$ in (27). When bounding $\Psi_k(t^*; \tau, \varepsilon^*) \geq c_L$ so as to prevent that $\Psi_k(p; \tau, \varepsilon^*) \rightarrow 0$, then the limit $\varepsilon^* \rightarrow 0$ in (27) will correspond to the metastable state of the SIS process,

$$y_{\pm}(p; \tau, 0) = \frac{1}{2} \left(1 - \frac{1}{\tau \mu_{N-k}} \right) \left\{ 1 + \sqrt{1 - \frac{\frac{c_L}{\tau \mu_{N-k}}}{1 - \frac{1}{\tau \mu_{N-k}}}} \right\}$$

which is precisely equal to the tanh-formula’s steady-state (22).